






# Combining Porous Se@SiO<sub>2</sub> Nanocomposites and dECM Enhances the Myogenic Differentiation of Adipose-Derived Stem Cells

Yu-Cheng Zhang <sup>1,2,\*</sup>, Yu-Xia Yang <sup>2,3,\*</sup>, Yu Liu<sup>4</sup>, Xi-Jian Liu <sup>5</sup>, Ji-Hang Dai<sup>2</sup>, Rang-Shan Gao<sup>2</sup>, Yang-Yang Hu <sup>2</sup>, Wen-Yong Fei <sup>2</sup>

<sup>1</sup>Clinical Medical College, Dalian Medical University, Dalian, 116044, People's Republic of China; <sup>2</sup>Department of Orthopedics and Sports Medicine, Northern Jiangsu People's Hospital, Affiliated to Yangzhou University, Yangzhou, 225001, People's Republic of China; <sup>3</sup>Clinical Medical College, Yangzhou University, Yangzhou, 225001, People's Republic of China; <sup>4</sup>Department of Orthopedics, Wuxi Ninth People's Hospital Affiliated to Soochow University, Wuxi, 214062, People's Republic of China; <sup>5</sup>School of Chemistry and Chemical Engineering, Shanghai University of Engineering Science, Shanghai, 201620, People's Republic of China

\*These authors contributed equally to this work

Correspondence: Yu Liu, Department of Orthopedics, Wuxi Ninth People's Hospital Affiliated to Soochow University, Wuxi, 214062, People's Republic of China, Email 529717824@qq.com; Wen-Yong Fei, Department of Orthopedics and Sports medicine, Northern Jiangsu People's Hospital, Yangzhou, 225001, People's Republic of China, Tel +86 180 5106 1779, Email sbydyx105@163.com

**Background:** Volumetric Muscle Loss (VML) denotes the traumatic loss of skeletal muscle, a condition that can result in chronic functional impairment and even disability. While the body can naturally repair injured skeletal muscle within a limited scope, patients experiencing local and severe muscle loss due to VML surpass the compensatory capacity of the muscle itself. Currently, clinical treatments for VML are constrained and demonstrate minimal efficacy. Selenium, a recognized antioxidant, plays a crucial role in regulating cell differentiation, anti-inflammatory responses, and various other physiological functions.

**Methods:** We engineered a porous Se@SiO<sub>2</sub> nanocomposite (SeNPs) with the purpose of releasing selenium continuously and gradually. This nanocomposite was subsequently combined with a decellularized extracellular matrix (dECM) to explore their collaborative protective and stimulatory effects on the myogenic differentiation of adipose-derived mesenchymal stem cells (ADSCs). The influence of dECM and NPs on the myogenic level, reactive oxygen species (ROS) production, and mitochondrial respiratory chain (MRC) activity of ADSCs was evaluated using Western Blot, ELISA, and Immunofluorescence assay.

**Results:** Our findings demonstrate that the concurrent application of SeNPs and dECM effectively mitigates the apoptosis and intracellular ROS levels in ADSCs. Furthermore, the combination of dECM with SeNPs significantly upregulated the expression of key myogenic markers, including MYOD, MYOG, Desmin, and myosin heavy chain in ADSCs. Notably, this combination also led to an increase in both the number of mitochondria and the respiratory chain activity in ADSCs.

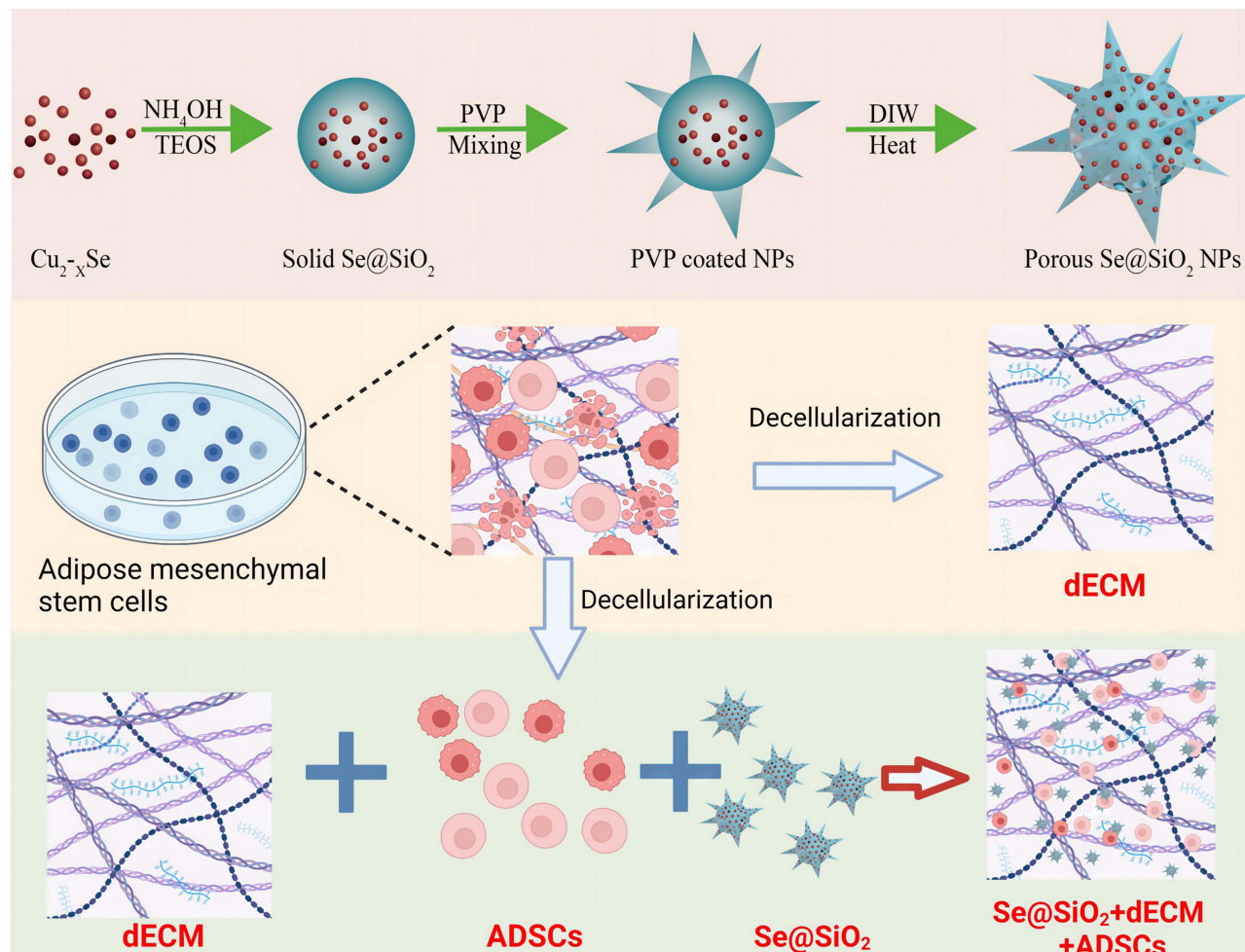
**Conclusion:** The concurrent application of SeNPs and dECM effectively diminishes ROS production, boosts mitochondrial function, and stimulates the myogenic differentiation of ADSCs. This study lays the groundwork for future treatments of VML utilizing the combination of SeNPs and dECM.

**Keywords:** porous Se@SiO<sub>2</sub> nanocomposite, SeNPs, adipose-derived mesenchymal stem cells, ADSCs, decellularized extracellular matrix, dECM, myogenic differentiation, mitochondria

## Introduction

As a crucial component of the human motor system, skeletal muscle possesses a regenerative capacity to a certain extent, capable of repair and regeneration after minor injuries. However, in specific scenarios resulting in severe muscle loss, such as volumetric muscle defects (VML), the extent of muscle loss surpasses the compensatory abilities of local stem cells and extracellular matrix (ECM). This frequently leads to impairment of limb function and permanent disability, imposing a substantial burden on both society and families.<sup>1</sup> Currently, effective treatments for VML remain limited.

## Graphical Abstract



While free skeletal muscle transplantation is a common clinical approach, its success is often hindered by a shortage of donors, and graft may not fully regenerate functional tissue.<sup>2</sup> In recent years, skeletal muscle tissue engineering (SMTE) has become a potential alternative to traditional VML surgery in regenerative medicine.<sup>3</sup>

Decellularized extracellular matrix (dECM) is a biomaterial obtained through physical or chemical means to eliminate cellular components while retaining extracellular matrix components.<sup>4</sup> dECM comprises proteins, glycosaminoglycans, proteoglycans, and various other matrix components present in the tissue. This composition mimics an optimal non-immune environment, featuring a natural three-dimensional structure along with a diverse array of bioactive components.<sup>5</sup> dECM scaffolds are basically free of DNA and antigenic epitopes, so they will not cause adverse immune reactions. Compared with the myoblasts cultured on tissue culture plastics, the myoblasts cultured on skeletal muscle dECM have higher growth rate and differentiation potential.<sup>6</sup> Based on the efforts of the majority of researchers, dECM has entered the clinical trial stage and provides the basis for other methods such as stem cells and drug delivery.<sup>7</sup> However, Garg et al found that using stem cell-free ECM scaffolds cannot recruit enough host stem cells in vivo alone to promote enough autologous fiber regeneration to achieve functional recovery.<sup>8</sup> Therefore, we believe that the successful design of skeletal muscle tissue engineering is inseparable from the assistance of stem cells.

The SMTE strategy involves the utilization of diverse stem cell types, including but not limited to mesenchymal stem cells, perivascular stem cells, and adipose-derived mesenchymal stem cells (ADSCs). ADSCs stand out as a particularly

appealing cell type due to their accessibility through a straightforward, high-yield isolation process. Subsequently, they can undergo rapid expansion and differentiation into myotubes, offering a means to evade host immune system influence and prevent rejection.<sup>9</sup> It has been proven that ADSCs can spontaneously display myogenic potential *in vitro* and have been detected as a potential donor cell to promote skeletal muscle regeneration *in vivo*.<sup>6</sup> In addition, in a mouse model of muscular dystrophy, after injecting ADSCs into injured skeletal muscle, the researchers found that ADSCs could regulate inflammation, increase angiogenesis, and regulate the expression of dystrophin.<sup>10</sup>

There are some limitations in the practical application of stem cell therapy, which usually requires effective expansion and culture *in vitro* in order to obtain a sufficient number of stem cells with differentiation potential.<sup>11</sup> However, the proliferation and differentiation potential of stem cells expanded *in vitro* may be low, and may even have a negative impact on their ability to promote skeletal muscle repair. Throughout the proliferation and differentiation of stem cells, the ongoing metabolic activities of cells result in the continual production of reactive oxygen species (ROS) by mitochondria.<sup>12</sup> Meanwhile, ROS play a regulatory role in cellular processes such as proliferation, migration, differentiation, and muscle contraction at the physiological level.<sup>13</sup> However, long-term exposure to excessive ROS may exceed the compensatory capacity of cells, resulting in inhibition of cell proliferation and differentiation, irreversible fibrosis and scarring in skeletal muscle, and eventually loss of muscle function.<sup>14</sup>

Selenium (Se) stands as a crucial trace element that contributes to the regulation of various physiological functions, including anti-inflammatory and immune responses. Additionally, it plays a significant role in the modulation of ROS levels.<sup>15,16</sup> However, high dose of Se is toxic to life, and low concentrations of Se sometimes cannot reach the effective concentration. Therefore, we have developed a kind of porous Se@SiO<sub>2</sub> nanocomposites (SeNPs) which can slowly release selenium.<sup>17</sup> This slow release and *in vivo* stability of SeNPs ensures their low toxicity and beneficial biosafety properties.<sup>18,19</sup> In previous studies, it was found that SeNPs have the ability to promote skeletal muscle regeneration.<sup>20</sup>

In this study, we incorporated dECM, a widely utilized material in regenerative medicine, building upon previous research. We innovatively merged SeNPs with dECM to investigate the impact of this composite structure on the myogenic differentiation of ADSCs. This exploration aims to establish a foundation for designing a robust and viable SMTE strategy for the treatment of VML.

## Materials and Methods

### Synthesis and Characterization of Porous SeNPs

The porous SeNPs were prepared as previously described.<sup>17,21</sup> In summary, the initial step involved the preparation of Cu<sub>2-x</sub>Se nanocrystals. Subsequently, a combination of n-hexane, n-hexanol, Triton X-100, deionized water, and tetraethyl orthosilicate was introduced. The addition of ammonium hydroxide facilitates the generation of [Cu (NH<sub>3</sub>)<sub>4</sub>]<sup>2+</sup>. The utilization of oxygen serves to oxidize Se<sup>2-</sup>, leading to the formation of selenium quantum dots (QDs). Silica-coated selenium QDs were then created through the hydrolysis of orthosilicate in an alkaline environment, resulting in the formation of solid SeNPs. These solid SeNPs underwent coating with PVP and subsequent etching in hot water to induce the development of porous structures. The characterization of SeNPs was carried out using a D/max-2550 PC XRD (Cu-K $\alpha$  radiation; Rigaku; Tokyo, Japan) and a transmission electron microscope (TEM, JEM-2100F).

### Cell Culture

The use of animals in this study was approved by the Animal Ethics Committee of Yangzhou University and was carried out in strict accordance with the “Public Health Service Policy on Humanitarian feeding and use of Experimental Animals” of American Public Health Service. ADSCs were sourced from Sprague-Dawley (SD) rats. In summary, humane euthanasia was performed on adult SD rats, and subsequent meticulous removal of blood vessels, fascia, and other tissues ensued using ophthalmic scissors and tweezers. Excision of adipose tissue followed, with digestion utilizing 0.1% collagenase type II (SCR103, Sigma, USA) at 37°C for 45 min. The resultant mixture was subjected to filtration using 200- $\mu$ m mesh filters, and the obtained filtrate was collected and centrifuged at 250 g for a duration of 5 min. Subsequently, the particles were resuspended in a complete medium and then transferred into a plastic cell culture flask. The cells were cultured in Dulbecco’s modified Eagle medium (DMEM)/F-12 medium (HyClone, Logan City, UT, USA)

supplemented with 10% fetal bovine serum (FBS) (Gibco, Grand Island, NY, USA) and 1% penicillin and streptomycin. This cultivation process was upheld at 37°C within a 5% CO<sub>2</sub> incubator. ADSCs from the third passage were employed for cell identification, dECM preparation, and subsequent experiments.

## Preparation of dECM Deposited by ADSCs

Tissue culture polystyrene (TCPS) plates underwent treatment with 0.2% gelatin (Sigma-Aldrich, St. Louis, MO, USA) at 37°C for 1 hr, followed by exposure to 1% glutaraldehyde (Sigma-Aldrich) and 1 M ethanolamine (Sigma-Aldrich) for 30 min at room temperature. After the removal of excess ethanolamine, the plates underwent three washes with phosphate-buffered saline (PBS). Subsequently, a growth medium was added, and the medium color was observed. If the medium turned purple, the plates were rinsed repeatedly until the medium returned to its normal color. ADSCs were cultured on pre-treated plates in a growth medium until reaching 90% confluence. Following that, 100-μM L-ascorbic acid was added for additional 7 days. To obtain decellularized extracellular matrix (dECM), cells were cultured in extraction buffer (0.5% Triton X-100 and 20 mM NH<sub>4</sub>OH in PBS, pH 7.4) at 37°C for 5 min. The dECM was washed with PBS three times to eliminate residual extraction buffer and then stored under sterile conditions at 4°C.<sup>22</sup>

## In vitro Safety of SeNPs

The in vitro safety assessment of porous SeNPs involves evaluating their inhibitory effect on the proliferation of ADSCs. ADSCs were initially seeded at a density of 1×10<sup>5</sup> cells per well in a flat-bottomed 48-well plate and cultured at 37°C with 5% CO<sub>2</sub> for 24 hr. Following this incubation period, the cells were exposed to varying concentrations of porous SeNPs (0–180 μg/mL). The subsequent day, ADSC proliferation was assessed using the MTT assay (Sigma, Saint Louis, MO, USA). In summary, each well was treated with MTT working solution for 4 hr, followed by a 30-min incubation with dimethyl sulfoxide. The absorbance was then measured at 492 nm using a miniature flat-panel reader (Thermo Fisher Scientific, MK3 type, Multiskan GO, Waltham, MA, USA).

At the same time, the proliferation and death of cells were observed by living dead cell staining on the 1st, 3rd, and 7th day of cell culture. Green dye can penetrate into the cell membrane of living cells, while red dye staining cannot pass through the cell membrane and can only label dead cells. In short, the cell sample was obtained on a specified number of days, diluted and added to the cell petri dish according to the instructions of calceinAM/PIkit (Biovision, CA, USA), and 30 min was incubated and washed with PBS. The ratio of living cells to dead cells was observed by fluorescence microscope (OlympusIX71, Olympus, Tokyo, Japan). The ratio of living cells to dead cells was calculated using ImageJ software.

## Myogenic Differentiation Induction of ADSCs

ADSCs were seeded in a 6-well plate at 4×10<sup>5</sup> cells/cm<sup>2</sup> and divided into six treatment groups: blank, Pentaazacytidine (5-Aza), 5-Aza + dECM, 5-Aza + Se@SiO<sub>2</sub> and 5-Aza + dECM + Se@SiO<sub>2</sub>. ADSCs were cultured in DMEM (Thermo Fisher) with 10 μM 5-Aza and 40 μg/mL Se@SiO<sub>2</sub>. We found that myotubules were abundant on the seventh day of ADSCs induced myogenic differentiation, so subsequent myogenic related tests were carried out on the seventh day to collect cell samples.

## Electron Microscopic Observation of dECM and Cells

For observing dECM, the dECM sample was fixed with 2.5% glutaraldehyde and dehydrated with an increase in ethanol concentration (50%, 75%, 80%, 95%, and 100%). The morphology of dECM samples was analyzed by scanning electron microscope (HT7700; Hitachi Hi-Tech, Tokyo, Japan).

For cultured cell samples, the conventional sample preparation process was adopted, including dehydration, immersion, embedding, ultra-thin section, and heavy metal staining. The morphology of mitochondria was observed by transmission electron microscope (Hitachi HT7700, Tokyo, Japan) at an accelerated voltage of 220kV.

## Enzyme-Linked Immunosorbent Assay (ELISA)

Rat IGF-1 and TGF- $\beta$  ELISA kits were purchased from Yu Bo Biotech (Shanghai, China). The expression levels of IGF-1 and TGF- $\beta$  in cell culture supernatants were assessed in accordance with the manufacturer's protocol. All tests were carried out three times.

## Detection of Mitochondrial ROS

Cell samples were obtained following a 7-day induction period. For the preparation of a MitoSOX Red Mitochondrial Superoxide Indicator solution (MitoSOX Red), 13  $\mu$ L of dimethyl sulfoxide was added to 50  $\mu$ g of the indicator (Yeasen), creating a 5-mM storage solution. This storage solution was then diluted 1000-fold with Hank's balanced salt solution, resulting in a final concentration of 5  $\mu$ M. The working solution (1–2 mL) was applied to cells growing on the climbing sheet, ensuring full coverage. Subsequently, cells were cultured at 37°C in the dark for 10 min, followed by counterstaining with Hoechst dye for additional 5 minutes. The prepared slide was sealed, and images were captured using a laser confocal microscope (Leica, TCS SP5).

## Evaluation of Mitochondrial Respiratory Chain Complex and Catalase Activities

The assessment of mitochondrial respiratory chain (MRC) activities entailed the use of both the MRC Complex Activity Assay Kit (Solarbio) and the ATP Synthetase Activity Assay Kit (YBio), adhering to the guidelines provided by the manufacturer. MRC activities were appraised via a colorimetric assay at 340, 550, and 450 nm, specifically targeting MRC complex I, MRC complex III, and ATP synthetase, respectively. The unit enzyme activity was quantified in terms of nmol/min/mg protein.

The evaluation of catalase activity was conducted using a readily available assay kit (Solarbio) in accordance with the provided guidelines. The preparation of protein samples involved lysing, and the total lysate protein concentration was determined through a BCA protein assay kit (Beyotime). Subsequently, each lysate was mixed with a colorimetric assay substrate solution from the kit and incubated at room temperature for a duration of 10 min. The absorbance at 405 nm was subsequently measured using a microplate reader (Thermo, MK3) along with a standard curve for reference.

## Immunofluorescence Staining

The dECM underwent fixation in 4% paraformaldehyde (Richjoint, Shanghai, China), followed by PBS washing, permeabilization with 1% Triton X-100 (Richjoint, Shanghai, China) for 15 min, and blocking in 5% FBS (Hyclone) for additional 15 minutes. Subsequently, the fixed dECM was subjected to incubation with appropriately diluted primary antibodies against type I collagen (Proteintech), type III collagen (Proteintech), fibronectin (Proteintech), and laminin (Abcam). Following a PBS rinse, the dECM was then incubated with Cy3-labelled goat anti-mouse IgG (Proteintech). Fluorescence images were captured using a confocal microscope (Leica, TCS SP5).

For intracellular staining, ADSCs underwent PBS washing, followed by permeabilization with 1% Triton X-100 (Richjoint, Shanghai, China) for 30 min and subsequent blocking in 5% FBS (Hyclone) for 5 min. Subsequently, the cells were subjected to staining with primary antibodies against MHC (Thermo Fisher Scientific), myosin (Proteintech), and desmin (Proteintech), followed by Cy3-labelled goat anti-mouse IgG (H + L). Finally, Hoechst stain (Beyotime Biotechnology) was applied to the cells, and the observation was conducted using a confocal microscope (Leica, TCS SP5).

## Western Blot Analysis

ADSCs were seeded in a 6-well plate at a density of  $4 \times 10^5$  cells/cm<sup>2</sup>. Following a 7-day myogenic induction, the ADSCs were washed thrice with PBS and lysed using lysis buffer (Biotech Well, Shanghai, China) supplemented with protease inhibitors (Biotech Well), phosphatase inhibitors (Biotech Well), and phenyl methane sulfonyl fluoride (Biotech Well). Protein concentrations were determined using the BCA protein assay kit (KGBCA). Equal protein amounts from each extract were denatured, separated on a 30% polyacrylamide gel (Sinopharm), and subsequently transferred to a polyvinylidene fluoride membrane (Millipore). The membrane was then incubated with diluted primary antibodies against SOD1 (Proteintech, 1:5000), MyHC (ThermoFisher, 1:500), MYOD (Proteintech, 1:5000), and GAPDH

(Proteintech, 1:5000) overnight at 4°C. Following this, membranes were exposed to the corresponding secondary antibody (goat anti-mouse IgG (H + L), Proteintech, NE, USA) at room temperature for 1 hr. Finally, protein bands were visualized using an enhanced chemiluminescence solution (Dingguo, Beijing, China), and ImageJ software was employed for band analysis. The protein expression is quantified by the normalized protein-to-GAPDH ratio.

## Statistical Analysis

Each experiment was carried out on at least three occasions. Qualitative data were obtained from a minimum of three independent experiments. The presentation of quantitative or semiquantitative data includes the mean  $\pm$  SD and under-vent analysis using GraphPad Prism 6. Data were subjected to one-way analysis of variance and Student's unpaired *t*-test. Statistical significance was defined as a *p*-value <0.05.

## Results

### Characterization of Porous SeNPs

Porous SeNPs synthesis as described in our previous study.<sup>17,23</sup> We used TEM to assess the morphological characteristics and sizes of the SeNPs. The nanocomposite diameter was approximately 55 nm, whereas the plentiful small QDs were dispersed in the region of about 5 nm (Figure 1B-D). After etching in the hot water, Se@SiO<sub>2</sub> formed a porous structure, which allowed the SeNPs to continuously release from the nanocomposites. The XRD pattern was used to assess the phase structure of the SeNPs. Many well-defined characteristic peaks were identified from solid SeNPs demonstrating a hexagonal phase, referenced by the standard selenium phase (JCPDS card no 65–1876; Figure 1A). The XRD pattern of the solid SeNPs showed an increase in the low angle region, which may be attributable to silica. The above results demonstrated that porous Se@SiO<sub>2</sub> nanospheres had been successfully prepared.

For safety and effectiveness, we then measured their toxicity *in vitro*. As shown in (Figure 1E), the concentration of more than 80  $\mu$ g/mL had no significant effect on cell proliferation. Finally, we chose the concentration of 40 as the working solution concentration of the follow-up experiment, because this concentration could obviously promote the proliferation of cells.

### Evaluation of dECM Deposited by ADSCs

We then stimulated ECM production by ADSCs by adding 250- $\mu$ M L-ascorbic acid and culturing for 7 days. The precipitated ECM was decellularized with TritonX-100, NH<sub>4</sub>OH and DNase I to remove cells and DNA residues. Type I collagen, type III collagen, fibronectin, and laminin were identified using IF staining in the dECM structure (Figure 2A). SEM images taken at 15,000 $\times$  and 30,000 $\times$  show that the structure of dECM is reticulate and that the lattice was composed of nanofibers and small bundles of collagen fibers (Figure 2B). The results of ELISA showed that there was no significant change in the contents of transforming growth factor- $\beta$  and insulin-like growth factor-1 in the supernatant of ECM before and after decellularization, indicating that part of the growth factors were successfully retained in the decellularized extracellular matrix (Figure 2C).

### Porous SeNPs Combined with dECM Reduces the Death of ADSCs

To investigate the effect of porous SeNPs and dECM on the proliferation of ADSCs, ADSCs were inoculated into cell culture dishes coated or uncoated with dECM at a cell density of  $5 \times 10^4$  cells/cm<sup>2</sup>. During the 7-day culture period, the medium containing porous SeNPs was changed every 3 days, and ADSCs was identified by IF staining. The high expression of CD44 and CD90 originated from stem cells, while the low expression of CD31 and CD45 excluded epidermal cells and vascular endothelial cells, respectively (Figure 3A). At the same time, the ADSCs successfully extracted from our previous studies has the ability of obvious three-line differentiation,<sup>24</sup> indicating that our extracted ADSCs meets the standards set by the International Society for Cell Therapy. We found that the SeNPs in the culture medium successfully entered the cells, and the release and accumulation of SeNPs in the cells was observed by transmission electron microscope on the 7th day of culture (Figure 3B). This is consistent with our previous observation through confocal microscopy that fluorescence-labeled SeNPs successfully entered the cells to exert biological effects.<sup>25</sup>

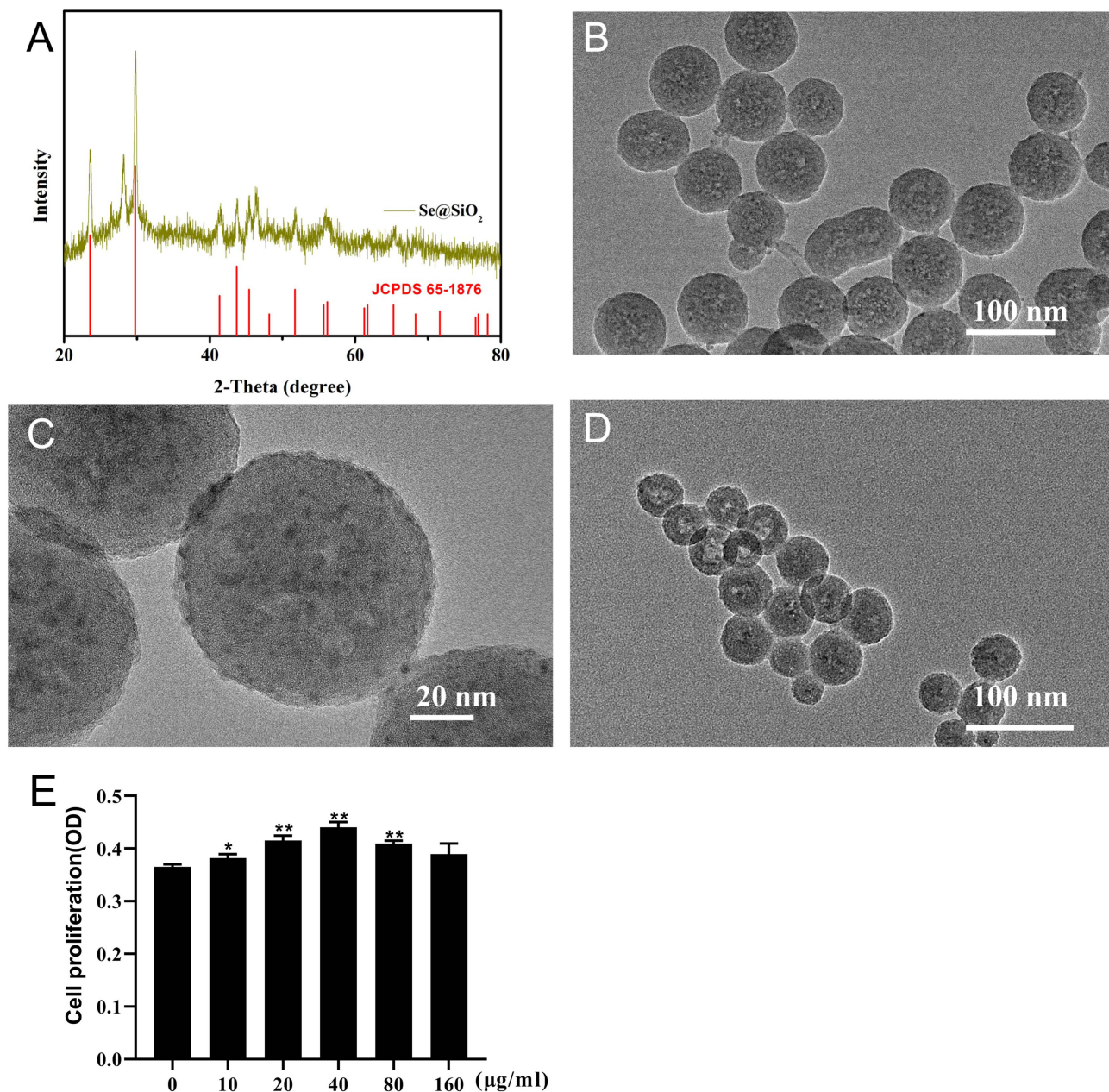


**Figure 1** Characterisation of the solid and porous SeNPs.

**Notes:** (A) XRD pattern of the solid SeNPs and the standard selenium nanocrystals (JCPDS card no:65–1876). (B) Medium- and (C) high-magnification TEM images of solid SeNPs. (D) TEM images of porous SeNPs. (E) ADSC viability following treatment with multiple porous SeNPs concentrations for 24 h. Data are expressed as mean  $\pm$  SD (n = 3). \*p < 0.05, \*\*p < 0.01.

The living cells and dead cells were stained on the 1st, 3rd, and 7th day of culture. The results showed that compared with the untreated control group, the change trend of each group was the same at these time points, and the proportion of dead cells increased after induction with 5-Aza, but decreased significantly after treatment with dECM and porous SeNPs (Figure 3C and D).

## Porous SeNPs Combined with dECM Promote ADSCs Myogenic Differentiation

Next, we evaluated whether porous SeNPs and dECM could promote the myogenic differentiation of ADSCs. ADSCs were inoculated into dECM-coated or uncoated cell Petri dishes at  $5 \times 10^4$  cells/cm<sup>2</sup> and then cultured in a medium containing porous SeNPs (40 µg/mL). After 7 days of culture, the expression of myogenic related genes was detected by

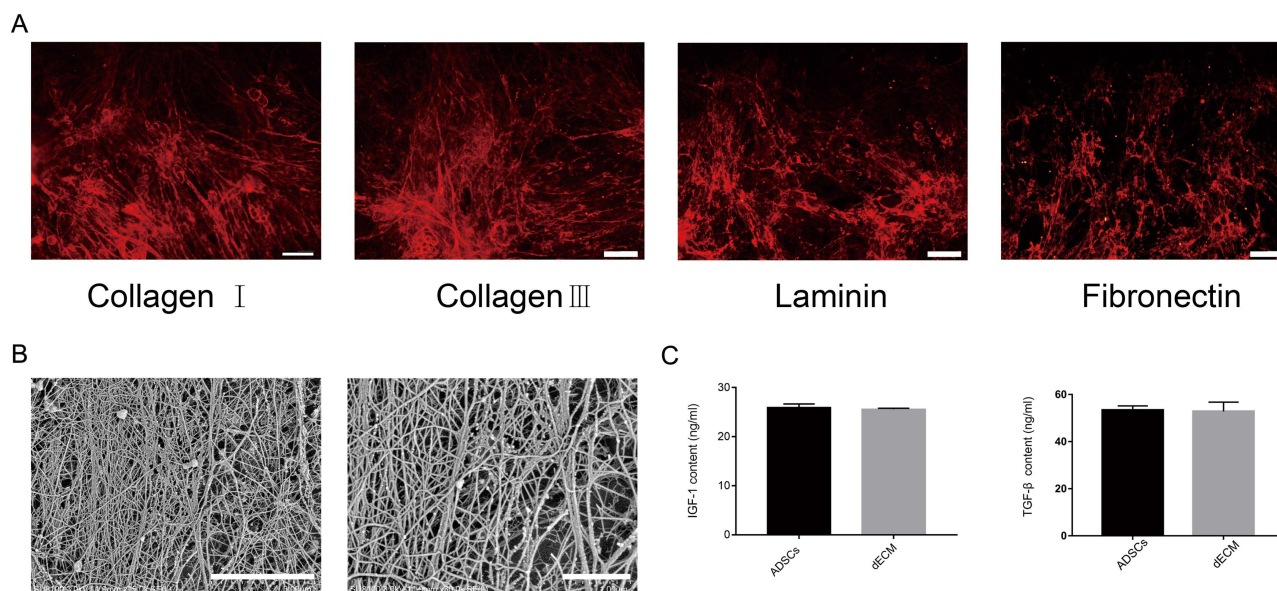


**Figure 2** Evaluation of dECM deposited by ADSCs.

**Notes:** (A) Representative images of IF staining identified type I and III collagens, fibronectin, and laminin in dECM; scale bar = 100  $\mu$ m. (B) SEM analysis indicates that dECM is made up of net-like lattices with small bundles of collagen fibers. Scale bar = 3 and 1  $\mu$ m. (C) ELISA detection of TGF- $\beta$  and IGF-I content before and after decellularisation.

IF staining and Western blotting. Compared with the normal control group, the expression of Desmin (Figure 4A and B), myosin (Figure 4C and D) and MHC (Figure 4E and F) increased significantly after 5-Aza was added to induce myogenic differentiation, and the cell differentiation was better. After treatment with dECM and porous SeNPs, the expression of MHC, myosin, and Desmin further increased. Therefore, the addition of dECM and porous SeNPs increases the degree of myotube formation. Western Blot qualitative data also validate this result (Figure 5A, D and E).

## Porous SeNPs Combined with dECM Reduce ROS Generation and Oxidative Stress Levels in ADSCs

In order to study the regulatory effect of porous SeNPs on ADSC oxidative stress (OS) and ROS production, MitoSOX Red was used to detect the level of ROS in mitochondria. Compared with the control group, the level of MitoSOX Red in cells increased after adding 5-Aza, while the level of MitoSOX Red decreased significantly after treatment with dECM and porous SeNPs, among which the decrease of dECM and porous Se@SiO<sub>2</sub> was the most obvious (Figure 5F–H). Through Western Blot, we observed a significant increase in the level of SOD1 in ADSCs treated with porous SeNPs and dECM. SOD1 is a protein that reflects the antioxidant capacity of cells. The higher its level, the stronger the antioxidant capacity of cells (Figure 5A and C). We used a commercially available assay kit to measure catalase activity (CAT). Results showed that compared with those in the normal control group, the levels of CAT significantly increased after the treatment with dECM and porous SeNPs; this increase was again most significant when both ECM and porous SeNPs were present (Figure 5B). These results further prove that porous SeNPs combined with dECM can reduce the production of ROS and improve the antioxidant capacity of ADSCs in the process of myogenesis.

## Porous SeNPs Combined with dECM Enhanced Mitochondrial Respiratory Function in ADSCs

To study the effects of porous SeNPs on the function of mitochondria, we looked at mitochondria function using Mito-Tracker (Figure 6A). The results showed that compared with the normal control group, the expression of Mito-Tracker (Figure 6C) and F-actin (Figure 6B) decreased after 5-Aza-induced myogenesis, while the expression of Mito-Tracker and F-actin increased significantly after dECM and porous SeNPs treatment, and this increase was most significant when



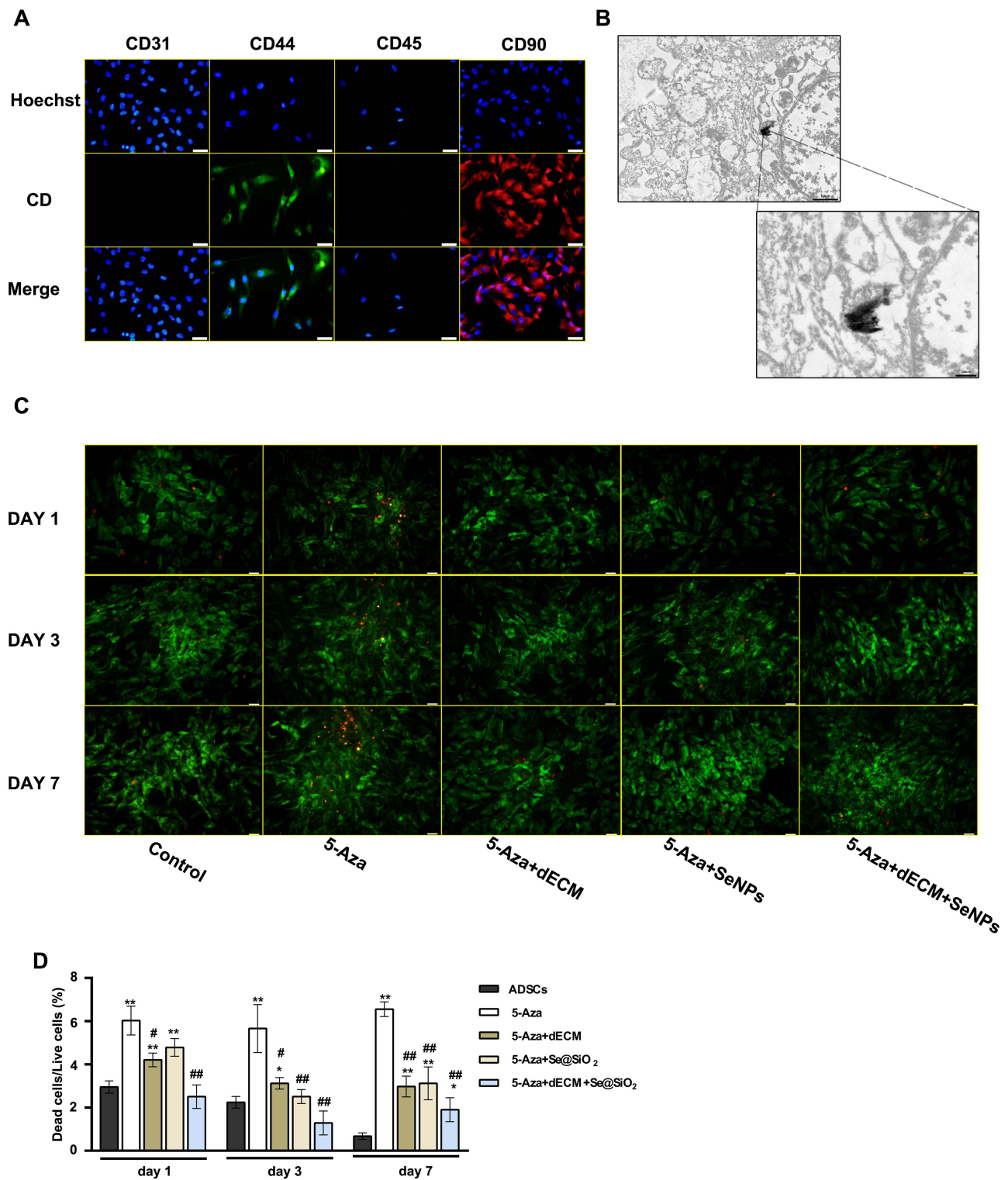


**Figure 3** Porous SeNPs combined with dECM reduces the death of ADSCs.

**Notes:** (A) IF staining showed that ADSCs had a high expression of CD44 and CD90 and low expression of CD31 and CD45; scale bar = 20 μm. (B) TEM images of porous SeNPs in cells; scale bar = 1000 and 250 nm. (C and D) Live and dead cell staining indicated that porous SeNPs promoted the proliferation of ADSCs. Living cells are green and dead cells are red; scale bar = 20 μm. Data are expressed as mean ± SD (n = 3). \*p < 0.05, \*\*p < 0.01 vs control group. #p < 0.05, ##p < 0.01 vs 5-Aza group.

dECM and porous SeNPs were added at the same time. Then, a variety of MRC activity detection kits were used to evaluate the mitochondrial function (Figure 6D–F). These results showed that, different from the normal control group, the activities of ATP synthase, MRC complex I and MRC complex III decreased after muscle induction with 5-Aza but

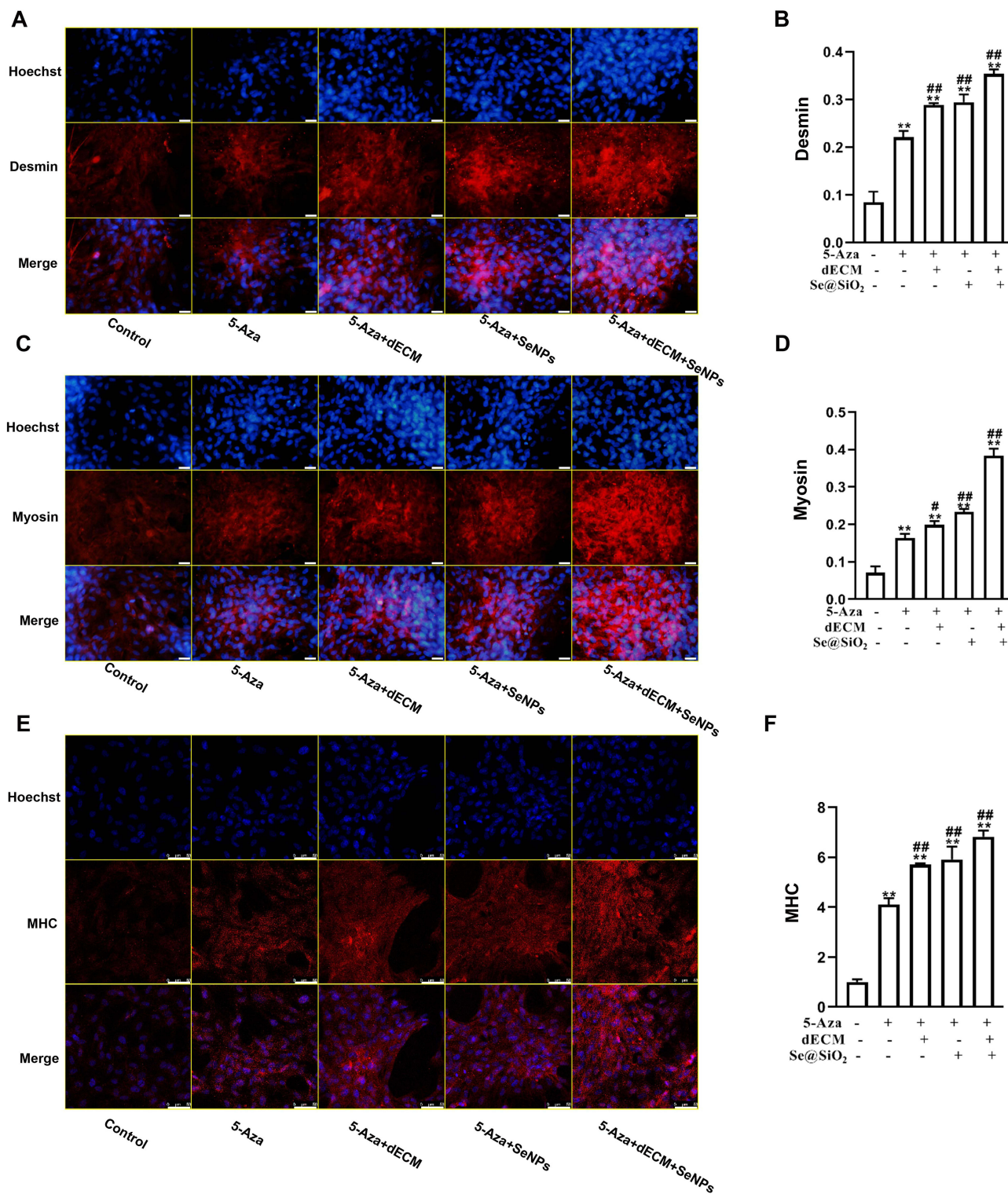


**Figure 4** Porous SeNPs combined with dECM promote adipose mesenchymal stem cell (ADSC) myogenic differentiation.

**Notes:** (A-F) Analysis of IF staining of ADSCs showed that the expression of Desmin (A), Myosin (C) and MHC (E) in ADSCs increased after treatment with porous SeNPs and that the degree of myotube formation was improved. Scale bar = 20 μm; Data are expressed as mean ± SD (n = 3). \*\*p < 0.01 vs control group. #p < 0.05, ##p < 0.01 vs 5-Aza group.

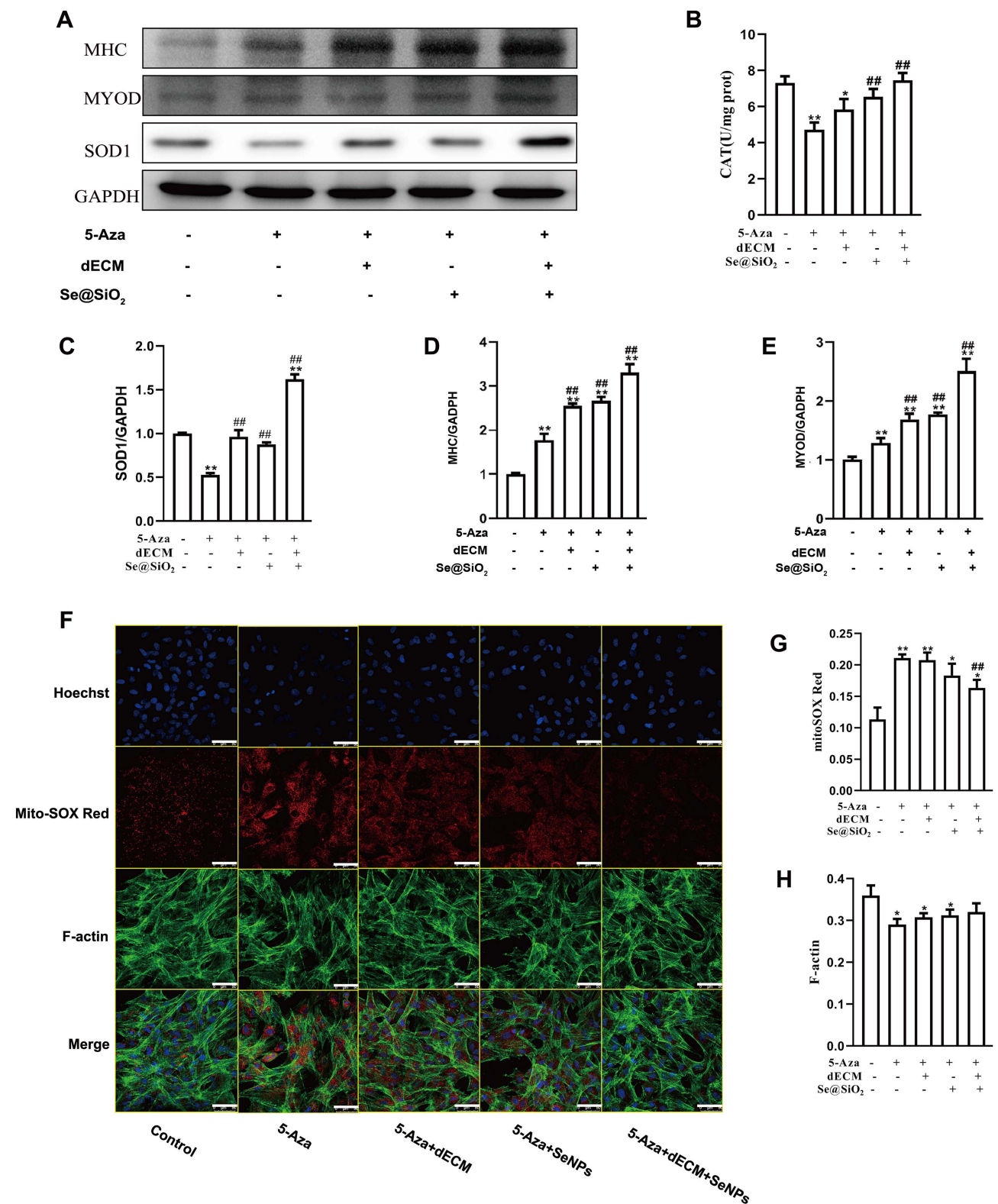


**Figure 5** Effects of Porous SeNPs combined with dECM on the expression of related proteins and ROS level during myoblast differentiation of ADSCs. **Notes:** (A) Western Blot was used to detect the level of MHC, MYOD, and SOD1 in ADSCs. (B) The levels of catalase activity in ADSCs. (C-E) Normalized data on the expression of SOD1, MHC, and MYOD proteins. (F-H) The levels of ROS in mitochondria were detected using MitoSOX Red. Levels of ROS in mitochondria decreased in varying degrees after the addition of dECM and porous SeNPs, and this decrease was most significant when both dECM and porous SeNPs were present simultaneously. Scale bar = 50 μm; Data are expressed as mean ± SD (n = 3). \*p < 0.05, \*\*p < 0.01 vs control group. ##p < 0.01 vs 5-Aza group.

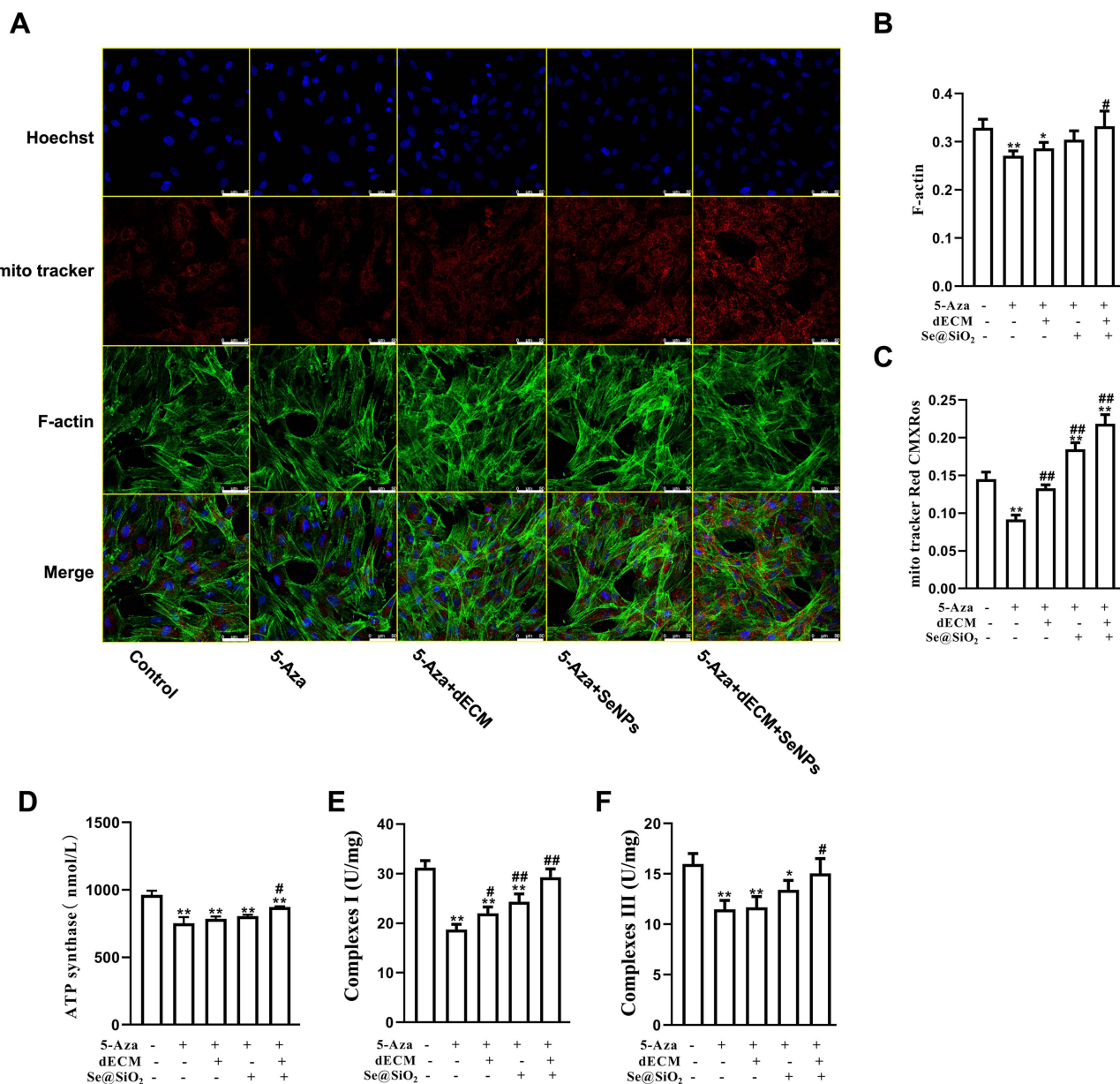


**Figure 6** Porous SeNPs increased mitochondrial number in ADSCs and promoted mitochondrial function.

**Notes:** (A-C) The number of intracellular mitochondria was detected using Mito-Tracker: the number of intracellular mitochondria increased in varying degrees after the treatment with dECM and porous SeNPs, and the increase was most significant when both dECM and porous SeNPs were added simultaneously. (D-F) Detection of mitochondrial function via ELISA: the levels of intracellular ATP synthase, MRC complex I and MRC complex III significantly increased after treatment with dECM and nano-selenium, with the most significant increase occurring when both dECM and nano-selenium were added simultaneously. Scale bar = 50 μm; All data are expressed as mean ± SD (n = 3). \*p < 0.05, \*\*p < 0.01 vs control group. #p < 0.05, ###p < 0.01 vs 5-Aza group.

increased significantly after treatment with dECM and porous SeNPs, which was most significant when ECM and porous SeNPs existed at the same time.

## Discussion

In this study, we observed that the synergy between porous SeNPs and dECM facilitated the myogenic differentiation of ADSCs, enhancing their antioxidant stress resilience. Furthermore, this combined approach augments both the quantity and respiratory function of ADSC mitochondria, mitigating the adverse impact of the 5-Aza myogenic inducer on cell proliferation to some extent. These findings present a novel and effective combination strategy for SMTE in the treatment of VML.

dECM contains natural ligands, ECM proteins, and growth factors found in skeletal muscle that are known to make a difference in cell chemotaxis and proliferation and in inflammatory responses and play an important role in myotube differentiation.<sup>9,26</sup> Our results also confirm this point of view. IF and Western blotting indicated that the levels of several proteins (MHC and MYOD) involved in regulating myogenesis in the ECM group were higher than those in the control group. The MTT assay also showed that ECM promoted the proliferation of ADSCs. However, previous studies have shown that there are a variety of uncertain factors in the single use of ECM in the experimental model, and ECM may not be able to achieve the desired effect after removing the cells. In a study conducted by Grag et al, the assessment of a syngeneic ECM scaffold in a rodent TA VML defect model revealed that, after 2 weeks of implantation, the scaffold elicited a proinflammatory response characterized by a significant presence of macrophages surrounding the implant.<sup>8</sup> Following an 8-week treatment period, there was a noticeable absence of myosin<sup>+</sup> muscle fibers, coupled with an augmented presence of collagen type I. Recent investigations employing a UBM ECM scaffold for addressing VML injuries in rodents and pigs indicated that the injuries treated with scaffolds exhibited restricted myogenesis and persistent functional deficiencies in the end stage.<sup>27,28</sup> We found that the addition of dECM could not significantly reduce the production of mitochondrial ROS, which was consistent with previous studies,<sup>29</sup> and SeNPs seemed to play a leading role in reducing the production of mitochondrial ROS.

Selenium is important in protecting cells from OS.<sup>30,31</sup> Selenium deficiency may lead to insufficient antioxidant capacity of tissues in certain diseases and multiple serious injuries.<sup>32</sup> Selenium has been reported to play a critical role in the proliferation and differentiation of MSCs.<sup>19,33</sup> Thus, we believe that the application of selenium as an antioxidant in promoting cell myogenic differentiation is vital. However, too much selenium can adversely affect cells and given the small gap between safety and toxicity,<sup>34</sup> we used nanoscale levels of selenium to reduce the risk of selenium poisoning. The optimal concentration of nano-selenium was determined through the MTT assay to ensure *in vitro* safety. In terms of OS, IF and Western blotting assays demonstrated a reduction in intracellular ROS production, accompanied by an increase in the levels of the antioxidant marker SOD1 after the addition of SeNPs. Initially, we employed an ECM to create a micro-3D environment for enhanced cell proliferation and differentiation. Interestingly, our observations revealed that ECM could also mitigate the oxidative stress response of cells to some extent, possibly attributed to the influence of various cytokines in the ECM. These findings led to the conclusion that porous SeNPs can enhance the ability of ADSCs to withstand ROS damage under oxidative stress conditions.

Excessive OS and antioxidant defence abilities are weakened, and dry loss and survival rate of mesenchymal stem cells are reduced. Excessive intracellular ROS is a typical manifestation of OS in damaged microenvironments. Overproduction of ROS and failure of antioxidant defence lead to a redox imbalance and increased OS.<sup>33,35</sup> Therefore, reducing OS and clearing excessive ROS may promote myogenesis.

We validate that the joint application of SeNPs and dECM effectively shields ADSCs from ROS and facilitates myogenic differentiation under ROS conditions. Our investigation pinpointed alterations in the levels of crucial myogenic signaling molecules, including MYOD, myosin, desmin, and MHC, through Western blotting and IF staining conducted at a concentration of 40  $\mu\text{g}/\text{mL}$  SeNPs. Notably, the porous SeNPs combined with dECM group exhibited a significant elevation in MYOD and MHC levels compared to the untreated group, and these levels were also augmented to a certain extent compared to groups treated with individual variables. In summary, our findings suggest that the combination of porous SeNPs and dECM holds promise for skeletal muscle repair by expediting myogenic differentiation through the fine-tuning of ROS production.

In the process of myogenic differentiation, mitochondria undergo many changes that are necessary for the progress of myogenic procedures.<sup>36,37</sup> In prior investigations, we established that the accumulated SeNPs could sustain mitochondrial ROS scavenging activity and enhance mitochondrial dynamics. In the current study, TEM observations indicated the material's entry into the cell, revealing a degree of agglomeration. Our IF and ELISA experiments demonstrated that SeNPs could stimulate an increase in mitochondrial numbers. Concurrently, the expression of MRC-related markers, including ATP synthase, RCC I, and RCC III, exhibited an elevation. The 5-Aza utilized in our experiments is a DNA methylation inhibitor known to promote cell myogenic differentiation while arresting the cell cycle. It is important to emphasize that changes in mitochondrial activity, as demonstrated in diverse studies, have the potential to modulate the expression of crucial regulators implicated in cell cycle withdrawal and terminal differentiation, including MYOD.<sup>38,39</sup>

Studies have shown that MRC complexes in cells can regulate cell cycle disorders.<sup>40</sup> Our findings indicate an augmentation in both the quantity and functionality of mitochondria following the introduction of nano-selenium and dECM. Additionally, the MTT test results demonstrated an increase in cell proliferation. Intriguingly, a recent study has furnished evidence suggesting that various sites within mitochondrial complexes play a role in ROS production during the differentiation process.<sup>41</sup> Notably, ROS production at MRC complex I progressively increases with differentiation.<sup>37,40</sup> Nevertheless, we have not established a definitive range of ROS content that can fulfill the requirements for cell myogenic differentiation without inducing excessive production and inhibiting differentiation. In this context, we illustrate that the amalgamation of porous SeNPs and dECM distinctly reinforces cellular resistance by fostering mitochondrial proliferation and enhancing respiratory function.

While our study has confirmed the effectiveness of SeNPs combined with dECM in protecting stem cells from myogenic differentiation through the modulation of mitochondrial activity and oxidative stress, there remains ample room for *in vivo* or clinical trials. Currently, the dECM we have prepared exhibits only a monolayer structure, with unstable physical and chemical properties, limiting its suitability for large-area or large-volume transplantation. Future efforts will focus on optimizing the structure of dECM and developing a stable composite dECM structure. Moreover, our ongoing research involves the inoculation of cells in a medium containing SeNPs and dECM. However, variations in SeNPs concentration across different locations may hinder their full impact on the cells. Consequently, further refinement of the structural characteristics of SeNPs is necessary. Our future objective is to engineer SeNPs capable of effectively adhering to dECM. We firmly believe that, through the continuous improvement of materials, the composite biomaterials comprising SeNPs and dECM can address the therapeutic needs of VML in the future.

## Conclusion

The prepared porous SeNPs exhibited a favorable impact on the myogenic differentiation and intracellular mitochondrial function of ADSCs, effectively mitigating the influence of ROS on ADSCs. Furthermore, the synergistic application of porous SeNPs and dECM significantly augmented the myogenic differentiation of ADSCs, mitigated the adverse effects of 5-Aza on the myogenic induction of ADSCs, and bolstered the antioxidant capacity and mitochondrial respiratory function of ADSCs. We contend that the combined utilization of porous SeNPs and dECM offers novel design concepts for SMTE, holding considerable potential for application in the treatment of VML.

## Author Contributions

All authors made substantial contributions to conception and design, acquisition of data, or analysis and interpretation of data; took part in drafting the article or revising it critically for important intellectual content; agreed to submit to the current journal; gave final approval for the version to be published; and agree to be accountable for all aspects of the work. Authors Yu-Cheng Zhang and Yu-Xia Yang made equal contributions to this study and should be regarded as co-first authors, the two authors are ranked in no particular order.

## Funding

The study was funded by the National Orthopaedic Sports Medicine and Rehabilitation Clinical Research Center under the project numbered 2021-NCRC-CXJJ-PY-07 and the scientific research project of Jiangsu Provincial Health Commission (M2021042). Furthermore, additional funding was extended through the Wuxi “Double Hundred” Young and Middle-aged Medical and Health Reserve Top-notch Talent Project, Medical and Public Health Technology Innovation and Application Project of Wuxi Science and Technology Bureau (N20202041).

## Disclosure

The authors confirm the absence of any conflicts of interest in this work.

## References

1. Patel KH, Talovic M, Dunn AJ, et al. Aligned nanofibers of decellularized muscle extracellular matrix for volumetric muscle loss. *J Biomed Mater Res*. 2020;108(6):2528–2537. doi:10.1002/jbm.b.34584
2. Gilbert-Honick J, Grayson W. Vascularized and Innervated Skeletal Muscle Tissue Engineering. *Adv Healthc Mater*. 2020;9(1):e1900626. doi:10.1002/adhm.201900626
3. McClure MJ, Cohen DJ, Ramey AN, et al. Decellularized Muscle Supports New Muscle Fibers and Improves Function Following Volumetric Injury. *Tissue Eng Part A*. 2018;24(15–16):1228–1241. doi:10.1089/ten.TEA.2017.0386
4. Zhang X, Chen X, Hong H, Hu R, Liu J, Liu C. Decellularized extracellular matrix scaffolds: recent trends and emerging strategies in tissue engineering. *Bioact Mater*. 2022;10:15–31. doi:10.1016/j.bioactmat.2021.09.014
5. Brown M, Li J, Moraes C, Tabrizian M, Li-Jessen NYK. Decellularized extracellular matrix: new promising and challenging biomaterials for regenerative medicine. *Biomaterials*. 2022;289:121786. doi:10.1016/j.biomaterials.2022.121786
6. Sicari BM, Dearth CL, Badylak SF. Tissue Engineering and Regenerative Medicine Approaches to Enhance the Functional Response to Skeletal Muscle Injury. *Anatomical Record*. 2014;297(1):51–64. doi:10.1002/ar.22794
7. Clinical application of an acellular biologic scaffold for surgical repair of a large, traumatic quadriceps femoris muscle defect - PubMed. Available from: <https://pubmed.ncbi.nlm.nih.gov/20608620/>. Accessed November 1, 2023.
8. Garg K, Ward CL, Rathbone CR, Corona BT. Transplantation of devitalized muscle scaffolds is insufficient for appreciable de novo muscle fiber regeneration after volumetric muscle loss injury. *Cell Tissue Res*. 2014;358(3):857–873. doi:10.1007/s00441-014-2006-6
9. Carnes ME, Pins GD. Skeletal Muscle Tissue Engineering: biomaterials-Based Strategies for the Treatment of Volumetric Muscle Loss. *Bioengineering*. 2020;7(3):85. doi:10.3390/bioengineering7030085
10. Pinheiro CH, de Queiroz JCF, Guimarães-Ferreira L, et al. Local injections of adipose-derived mesenchymal stem cells modulate inflammation and increase angiogenesis ameliorating the dystrophic phenotype in dystrophin-deficient skeletal muscle. *Stem Cell Rev Rep*. 2012;8(2):363–374. doi:10.1007/s12015-011-9304-0
11. Montarras D, Morgan J, Collins C, et al. Direct isolation of satellite cells for skeletal muscle regeneration. *Science*. 2005;309(5743):2064–2067. doi:10.1126/science.1114758
12. Radak Z, Torma F, Berkes I, et al. Exercise effects on physiological function during aging. *Free Radic Biol Med*. 2019;132:33–41. doi:10.1016/j.freeradbiomed.2018.10.444
13. Jones RM, Mercante JW, Neish AS. Reactive oxygen production induced by the gut microbiota: pharmacotherapeutic implications. *Curr Med Chem*. 2012;19(10):1519–1529. doi:10.2174/092986712799828283
14. García-Redondo AB, Aguado A, Briones AM, Salices M. NADPH oxidases and vascular remodeling in cardiovascular diseases. *Pharmacol Res*. 2016;114:110–120. doi:10.1016/j.phrs.2016.10.015
15. Cheng WH, Prabhu KS. Special Issue of “Optimal Selenium Status and Selenoproteins in Health. *Biol Trace Elem Res*. 2019;192(1):1–2. doi:10.1007/s12011-019-01898-x
16. Lee SC, Lee NH, Patel KD, et al. The Effect of Selenium Nanoparticles on the Osteogenic Differentiation of MC3T3-E1 Cells. *Nanomaterials*. 2021;11(2):557. doi:10.3390/nano11020557
17. Liu X, Deng G, Wang Y, et al. A novel and facile synthesis of porous SiO<sub>2</sub>-coated ultrasmall Se particles as a drug delivery nanoplatfrom for efficient synergistic treatment of cancer cells. *Nanoscale*. 2016;8(16):8536–8541. doi:10.1039/C6NR02298G
18. Zheng Z, Deng G, Qi C, et al. Porous Se@SiO<sub>2</sub> nanospheres attenuate ischemia/reperfusion (I/R)-induced acute kidney injury (AKI) and inflammation by antioxidative stress. *Int J Nanomed*. 2019;14:215–229. doi:10.2147/IJN.S184804
19. Li C, Wang Q, Gu X, et al. Porous Se@SiO<sub>2</sub> nanocomposite promotes migration and osteogenic differentiation of rat bone marrow mesenchymal stem cell to accelerate bone fracture healing in a rat model. *Int J Nanomed*. 2019;14:3845–3860. doi:10.2147/IJN.S202741
20. Porous Se@SiO<sub>2</sub> nanoparticles improve oxidative injury to promote muscle regeneration via modulating mitochondria - PubMed. Available from: <https://pubmed.ncbi.nlm.nih.gov/36331417/>. Accessed November 12, 2023.
21. Improved rotator cuff healing after surgical repair via suppression of reactive oxygen species by sustained release of Se | request PDF. Available from: [https://www.researchgate.net/publication/350315662\\_Improved\\_rotator\\_cuff\\_healing\\_after\\_surgical\\_repair\\_via\\_suppression\\_of\\_reactive\\_oxygen\\_species\\_by\\_sustained\\_release\\_of\\_Se](https://www.researchgate.net/publication/350315662_Improved_rotator_cuff_healing_after_surgical_repair_via_suppression_of_reactive_oxygen_species_by_sustained_release_of_Se). Accessed October 31, 2023.
22. Liu X, Zhou L, Chen X, et al. Culturing on decellularized extracellular matrix enhances antioxidant properties of human umbilical cord-derived mesenchymal stem cells. *Mater Sci Eng C*. 2016;61:437–448. doi:10.1016/j.msec.2015.12.090
23. Zhu Y, Deng G, Ji A, et al. Porous Se@SiO<sub>2</sub> nanospheres treated paraquat-induced acute lung injury by resisting oxidative stress. *IJN*. 2017;12:7143–7152. doi:10.2147/IJN.S143192
24. Fei W, Pang E, Hou L, et al. Synergistic Effect of Hydrogen and 5-Aza on Myogenic Differentiation through the p38 MAPK Signaling Pathway in Adipose-Derived Mesenchymal Stem Cells. *Int J Stem Cells*. 2023;16(1):78–92. doi:10.15283/ijsc21238
25. Mitochondria-Modulating Porous Se@SiO<sub>2</sub> Nanoparticles Provide Resistance to Oxidative Injury in Airway Epithelial Cells: implications for Acute Lung Injury - PubMed. Available from: <https://pubmed.ncbi.nlm.nih.gov/32280221/>. Accessed November 10, 2023.
26. Grasman JM, Zayas MJ, Page RL, Pins GD. Biomimetic scaffolds for regeneration of volumetric muscle loss in skeletal muscle injuries. *Acta Biomater*. 2015;25:2–15. doi:10.1016/j.actbio.2015.07.038
27. Ostrovidov S, Hosseini V, Ahadian S, et al. Skeletal Muscle Tissue Engineering: methods to Form Skeletal Myotubes and Their Applications. *Tissue Eng Part B, Rev*. 2014;20(5):403–436. doi:10.1089/ten.teb.2013.0534
28. Aurora A, Roe JL, Corona BT, Walters TJ. An acellular biologic scaffold does not regenerate appreciable de novo muscle tissue in rat models of volumetric muscle loss injury. *Biomaterials*. 2015;67:393–407. doi:10.1016/j.biomaterials.2015.07.040
29. Garg K, Ward CL, Corona BT. Asynchronous inflammation and myogenic cell migration limit muscle tissue regeneration mediated by acellular scaffolds. *Inflamm Cell Signal*. 2014. doi:10.14800/ics.530
30. Srivastava D, Subramanian R, Madamwar D, Flora S. Protective Effects of Selenium, Calcium, and Magnesium Against Arsenic-Induced Oxidative Stress in Male Rats. *Archiv Indus Hygien Toxicol*. 2010;61(2):153–159. doi:10.2478/10004-1254-61-2010-1993
31. Kielczykowska M, Kocot J, Paździor M, Musik I. Selenium – a fascinating antioxidant of protective properties. *Adv Clin Exp Med*. 2018;27(2):245–255. doi:10.17219/acem/67222

32. Khurana A, Tekula S, Saifi MA, Venkatesh P, Godugu C. Therapeutic applications of selenium nanoparticles. *Biomed Pharmacother.* 2019;111:802–812. doi:10.1016/j.biopha.2018.12.146
33. Fatima S, Alfrayh R, Alrashed M, Alsobaie S, Ahmad R, Mahmood A. Selenium Nanoparticles by Moderating Oxidative Stress Promote Differentiation of Mesenchymal Stem Cells to Osteoblasts. *IJN.* 2021;16:331–343. doi:10.2147/IJN.S285233
34. Estevez H, Garcia-Lidon JC, Luque-Garcia JL, Camara C. Effects of chitosan-stabilized selenium nanoparticles on cell proliferation, apoptosis and cell cycle pattern in HepG2 cells: comparison with other selenospecies. *Colloids Surf B Biointerfaces.* 2014;122:184–193. doi:10.1016/j.colsurfb.2014.06.062
35. Chen H, Huang X, Fu C, et al. Recombinant Klotho Protects Human Periodontal Ligament Stem Cells by Regulating Mitochondrial Function and the Antioxidant System during H<sub>2</sub>O<sub>2</sub>-Induced Oxidative Stress. *Oxidative Med Cell Longevity.* 2019;2019:1–14. doi:10.1155/2019/9261565
36. Wagatsuma A, Sakuma K. Mitochondria as a Potential Regulator of Myogenesis. *Sci World J.* 2013;2013:1–9. doi:10.1155/2013/593267
37. Bhattacharya D, Scimè A. Mitochondrial Function in Muscle Stem Cell Fates. *Front Cell Dev Biol.* 2020;8:480. doi:10.3389/fcell.2020.00480
38. Bahat A, Gross A. Mitochondrial plasticity in cell fate regulation. *J Biol Chem.* 2019;294(38):13852–13863. doi:10.1074/jbc.REV118.000828
39. Rosca AM, Burlacu A. Effect of 5-Azacytidine: evidence for Alteration of the Multipotent Ability of Mesenchymal Stem Cells. *Stem Cells Dev.* 2011;20(7):1213–1221. doi:10.1089/scd.2010.0433
40. Chabi B, Hennani H, Cortade F, Wrutniak-Cabello C. Characterization of mitochondrial respiratory complexes involved in the regulation of myoblast differentiation. *Cell Biol Int* 2021;45(8):1676–1684. doi:10.1002/cbin.11602
41. Goncalves RLS, Watson MA, Wong HS, Orr AL, Brand MD. The use of site-specific suppressors to measure the relative contributions of different mitochondrial sites to skeletal muscle superoxide and hydrogen peroxide production. *Redox Biol.* 2020;28:101341. doi:10.1016/j.redox.2019.101341

International Journal of Nanomedicine

Dovepress

## Publish your work in this journal

The International Journal of Nanomedicine is an international, peer-reviewed journal focusing on the application of nanotechnology in diagnostics, therapeutics, and drug delivery systems throughout the biomedical field. This journal is indexed on PubMed Central, MedLine, CAS, SciSearch®, Current Contents®/Clinical Medicine, Journal Citation Reports/Science Edition, EMBase, Scopus and the Elsevier Bibliographic databases. The manuscript management system is completely online and includes a very quick and fair peer-review system, which is all easy to use. Visit <http://www.dovepress.com/testimonials.php> to read real quotes from published authors.

Submit your manuscript here: <https://www.dovepress.com/international-journal-of-nanomedicine-journal>